

# Grant-free transmissions based on successive interference cancellation in IoT

Asmad Bin Abdul Razzaque  
Department of Information Engineering,  
Electronics and Telecommunications (DIET)  
University of Rome Sapienza, Italy  
asmadbin.razzaque@uniroma1.it

Andrea Baiocchi  
Department of Information Engineering,  
Electronics and Telecommunications (DIET)  
University of Rome Sapienza, Italy  
andrea.baiocchi@uniroma1.it

**Abstract**—Advancements in the physical layer design are pushing towards a major re-design of multiple access schemes for Next Generation Wireless Communication Systems. Hence, we turn towards random multiple access. We use a general model to investigate the interplay between random multiple access protocols and physical layer functions, specifically Successive Interference Cancellation (SIC). We focus on the sum-rate metric, which has been shown to exhibit two local maxima as a function of the target Signal to Interference plus Noise Ratio (SINR) [1]. The contribution of this paper lies with assessing the sensitivity of the optimal sum-rate to the number of concurrent transmissions, transmission power setting, and imperfect interference cancellation. Furthermore, leveraging the understanding gained on sum-rate optimization, we define a sum-rate optimal adaptive algorithm, when the number of contending nodes varies with time.

**Index Terms**—Successive Interference Cancellation, multi-packet reception, massive multiple access, Slotted ALOHA, CSMA, grant-free.

## I. INTRODUCTION

The huge demand for dense object connectivity, ultra-low latency, and higher data rates is not compatible with dedicated spectrum band allocation for each individual connection. This is especially true in Machine-to-Machine (M2M) communications which is the cornerstone of Internet of Things (IoT) applications [2]. Grant-free multiple access targets this issue, typically resorting to contention based multiple access algorithms. Those algorithms have to face new challenges. As an example, 6G requirements encompass device density of 10 million/km<sup>2</sup> [3].

Key traffic characteristics of massive IoT applications are: mostly up-link (UL) traffic, very small transmit-data size per device, extremely high energy efficiency requirement, partially/fully autonomous communication, and most importantly sporadic transmission [4]. In the existing cellular network, each user requests a data transmission slot via a contention-based random access (RA) process, and this communication is usually referred to as grant-based communications. Massive IoT scenarios with a large density of partially/fully autonomous devices call for grant-free communications, where a device can transmit data on a shared channel as per their requirements [5]. NOMA is the key driving factor in grant-free communications. A possible path to implementing NOMA is to rely on advanced

physical layer functions that enable multi-packet reception and on contention resolution or contention mitigation offered by random access algorithms.

Random Access (RA) protocols, which are responsible for contention resolution in shared channels, lie at the core of current and future wireless transmission technologies. Slotted Aloha (SA) is a classic RA technique in which users send their bursts within slots in a distributed way. The average normalized throughput of classic SA cannot exceed the  $1/e$  limit due to collisions among simultaneous transmissions and to idle slots. Carrier Sense Multiple Access (CSMA) is known to break this limit, as long as channel sensing works. It has been widely adopted in wired and wireless Local Area Networks, e.g., it is the core algorithm for the distributed coordination function of WiFi at least up to IEEE 802.11ac and still plays a major role in the last WiFi version, IEEE 802.11ax. To improve the performance of classic random access protocols for next generation wireless systems requires advanced physical layer functions yielding effective Multi-Packet Reception (MPR).

In the rapidly evolving landscape of wireless communications, the potential of MPR along with Non-Orthogonal Multiple Access (NOMA) has garnered significant attention. These advancements promise to revolutionize wireless networks by enabling massive connectivity and improving spectral efficiency in a decentralized multiple access. The related work in this domain has explored the integration of MPR and NOMA into various random access protocols, sparking discussions about their benefits and implications [5]–[13].

In the quest for efficient wireless systems, a significant gap remains in understanding the interaction between multiple access protocols and advanced physical layer functions. While existing studies have touched upon the promise of these techniques [14], [15], a comprehensive analysis of their effects on connectivity, power allocation, and the balance between MAC and PHY layers is yet to be understood in detail. This paper aims to contribute such understanding, by providing a general modeling framework of RA with Successive Interference Cancellation (SIC) capable physical layer, thus enabling MPR. Presented results extend the analysis of our previous work [1]. We further investigate the system performance by modifying the adopted path loss model and by considering several alternative transmission power setting schemes. Performance evaluation

is focused on the sum-rate metric, aiming to explore the sensitivity of the maximum achievable sum-rate with respect to transmission power setting, number of contending nodes, imperfect interference cancellation.

We provide the following main original contributions:

- We highlight the sensitivity of the already identified two regimes in [1] with respect to number of transmitting nodes: (i) high spectral efficiency, where Channel Sensing Multiple Access (CSMA) outperforms Slotted ALOHA (SA) in terms of sum-rate and SIC give little contribution to system performance; and (ii) low spectral efficiency, where the effect of MAC protocol is marginal, and performance are dominated by SIC.
- We highlight sum-rate improvement in the low spectral efficiency regime, based on different transmission power setting schemes.
- We identify the impact of imperfect interference cancellation, showing that even 10% residual interference can significantly impair the maximum achievable sum-rate.
- We exploit the insight gained in the preceding analysis of sum-rate to define an adaptive algorithm to adjust key system parameters in a dynamic environment where the number of backlogged nodes varies over time. The adaptive algorithm guarantees stability of the channel, while maximizing the long-term average sum-rate.

The rest of the paper is organized as follows. Related work is discussed in Section II. Section III summarizes the modeling approach and the main assumptions. Expressions of the overall sum-rate are also introduced in Section III. Numerical results are provided in Section IV. Section V presents the dynamic optimization of sum-rate. Conclusions are drawn in Section VI, including future work directions.

## II. RELATED WORK

A need has been highlighted for the redesign of multiple access to support a massive number of devices, that send infrequent and short data packets, which cannot be effectively accommodated using orthogonal resources [5], [16], [17].

Recently, Non-Orthogonal Multiple Access (NOMA) has emerged to incorporate massive connectivity based on multi-user detection capabilities at the receiver. A paradigm shift is emerging from random access contention based to grant-free transmission [18], where users can transmit data whenever they want without scheduling any request, utilizing NOMA potential for massive machine type communication [5], [18], [19]. An extensive literature has been growing on new multiple access techniques [6]–[8], especially NOMA, for achieving high connectivity, low latency and few collisions.

A fundamental issue toward designing a grant-free transmission schemes exists from the receiver perspective, as the massive connectivity of devices at some point will result in great collisions due to limited decoding capability of the receiver. A smooth transition is needed from grant-based to grant-free transmission schemes [18]. In this regard, a semi-grant-free transmissions scheme is proposed recently, to enhance the access performance of Machine Type Communication

(MTC) devices. Semi-grant-free schemes offer a much more controllable system than the grant-free schemes which results in less overhead [20]. The adoption of semi-grant free transmission is driven by two primary factors in cellular systems. Firstly, it capitalizes on user coordination. Secondly, it promotes enhanced cooperation among users employing grant-free and grant-based methods, thereby optimizing the utilization of limited radio resources. As a result various semi-grant-free strategies have been proposed within the framework of Non-Orthogonal Multiple Access (NOMA) [18], [20]. One of them encompass both the grant-free and grant-based users, along with the base-station deployment. While scheduling the grant-base user transmissions, the base station broadcasts a threshold for grant-free users and anyone who satisfies the threshold number can transmit directly in grant-free mode [20]. In continuation to this authors in [21] invoked the stochastic geometry approaches to enhance the spectral efficiency. A dynamic threshold protocol proposed in [21] gives grant-free users much more flexibility in connectivity as compared to [20].

Furthermore, in [10], [22], the performance of grant-free access is investigated by incorporating ALOHA or slotted-ALOHA protocols with power-domain NOMA. Power-Domain Non-Orthogonal Multiple Access (PD-NOMA) regulate transmission power levels which as result allows Successive Interference Cancellation to work effectively [23]. To improve the performance of Slotted ALOHA-based systems for the next generation of wireless technology, a different approach at the physical level has been proposed which exploits the Multi-Packet Reception at the receiver to enhance the sum-rate [24]–[26]. The work in [27] highlights the significance of adaptive transmission probabilities, fairness considerations, and the impact of channel state information on the network throughput. This study is further extended by analyzing two SIC receiver models: ordered SIC and unordered SIC [14]. The main contribution involves the understanding of implications of SIC receivers and their comparison with the capture model, along with shedding light on rate losses due to uncoordinated transmissions in Slotted Aloha networks [14]. A few additional works delve into power allocation strategies within random access protocols [12], [13]. The evolving landscape is evident as studies explore SIC's network-level impacts [10], [11], [15], prompting a reconsideration of upper-layer protocols for IoT scenarios.

Most of these studies are primarily focused towards PHY layer or the MAC layer, and the existence of different regimes in sum-rate is not identified in any of these in terms of MAC, PHY layer perspective. Here we present an in-depth investigation of achievable sum rate based on a general modeling approach introduced in our previous work [1], where PHY and MAC are jointly analyzed.

## III. SYSTEM MODEL

In this section we summarize the system model from [1]. The deterministic path loss model and transmission power level settings 2 and 3 presented below are new with respect to the model defined in [1].

### A. Spectral Efficiency, SINR and Path Loss model

We consider  $n$  nodes sharing a communication channel of bandwidth  $W$  and spectral efficiency  $\eta$  (bits/sec/Hz). Additive background noise as well as interference is modeled as a Gaussian process. The Signal to Interference plus Noise Ratio (SINR)  $\Gamma$  at the receiver side is given by,

$$\Gamma = \frac{GP_{tx}}{P_N + P_I} \quad (1)$$

where  $G$  is the path gain of the link between the transmitter and the receiver,  $P_{tx}$  is the transmitted power level,  $P_N$  is the background thermal noise power level, and  $P_I$  is the interference power level.

The spectral efficiency  $\eta$  is related to the required SINR level, denoted with  $\gamma$ , as follows:

$$\eta = \log_2(1 + \gamma) \quad (2)$$

In the following we assume that a packet is decoded successfully if the average SINR at which the packet is received exceeds the required SINR level, i.e., if it is  $\Gamma \geq \gamma = 2^\eta - 1$ .

The path gain  $G$  is modeled as  $G = G_d G_s G_f$ , i.e., it is the product of a deterministic component  $G_d$ , accounting for distance between the transmitter and the receiver, a log-normal random component  $G_s$ , accounting for shadowing due to obstacles, and a negative exponential random component  $G_f$ , accounting for multi-path Rayleigh fading.

The Two-Ray Ground path loss model from [28] is used to account for the deterministic component  $G_d$ . Model parameters include the distance between the transmitter and the receiver, height of the transmitter, height of the receiver, and the carrier frequency. This model is especially apt to represent the path loss in outdoor environments, with line-of-sight reception as well as reflected e.m. field from the ground.

The shadowing  $G_s$  is assumed to remain the same for a given node throughout its communication activity. It is given by  $G_s = 10^{\sigma_s Z/10}$ , where  $\sigma_s$  is the shadowing standard deviation in dB and  $Z$  is a standard Gaussian random variable (zero mean, unit variance).

The fading  $G_f$  depends on variability of the propagation scenario. It is sampled from a negative exponential probability distribution with unit mean, independently packet by packet. Hence, it is  $\mathcal{P}(G_f > x) = e^{-x}$ ,  $x > 0$ .

The background thermal noise power level,  $P_N$ , is given by  $P_N = F_N N_0 W$ , where  $F_N$  is the noise figure and  $N_0 = -174$  dBm/Hz is the thermal noise power spectral density.

The transmission time of a packet (including overhead) is denoted with  $T$ . Let  $L$  denote the packet length. Then, it is

$$T = \frac{L}{W \log_2(1 + \gamma)} \quad (3)$$

In the ensuing analysis of the sum-rate, we assume that the  $n$  nodes are saturated, i.e., they have always packets ready to send. Non saturated nodes are considered in Section V.

### B. Power Control

Nodes are scattered uniformly at random within a maximum distance  $R$  from a Base Station (BS).

Power dynamic range is limited to the interval  $[P_{tx,\min}, P_{tx,\max}]$ . We have used three different settings of power control, to compare how different settings affect sum-rate. The considered settings are as follow:

- *Scheme 1: same received power level.* Each node aims at achieving an average received power level  $P_{rx} = P_0$ , same for all nodes. Equivalently, the Signal-to-Noise Ratio (SNR) level targeted by each node is  $S_0 = P_0/P_N$ . This target is pursued under the constraint of a finite power dynamic range. The node has to estimate its deterministic and shadowing path gain components, e.g., by means of periodic pilot tones sent by the BS. Then, the node sets its transmission power level so as to compensate those two components. Let  $G_i$  be the estimated average path loss of node  $i$  (deterministic path loss plus shadowing). Then,

$$P_{tx,i} = \max \left\{ P_{tx,\min}, \min \left\{ P_{tx,\max}, S_0 \frac{P_N}{G_i} \right\} \right\} \quad (4)$$

The value of  $S_0$  is chosen as follows. The received SNR for a given packet, undergoing fast fading gain  $G_f$  and in case of no interference (single transmitter), is  $S = S_0 G_f$ . Packet decoding is successful, if  $S > \gamma$ , i.e., if  $G_f > \gamma/S_0$ . Since  $G_f$  is a negative exponential random variable with mean 1, the probability of successful decoding, in case of a single transmitter is  $e^{-\gamma/S_0}$ . The level  $S_0$  is set so that this probability be at least  $1 - \epsilon$ , i.e.,  $S_0 = -\gamma/\log(1 - \epsilon)$ .

- *Scheme 2: tx power proportional to distance.* The transmission power level  $P_{tx}$  is adjusted based on the position of the node. Let  $d_i$  be the distance of node  $i$  from the BS. Then, the transmission power of node  $i$  is set as

$$P_{tx,i} = \max \left\{ P_{tx,\min}, \frac{d_i}{R} P_{tx,\max} \right\} \quad (5)$$

where  $R$  is the maximum distance at which a node is allowed to associate with the given BS. The average received power level will not be the same for all nodes. While this unequal level of received power is generally harmful in case of multiple access, it is expected to be beneficial to improve SIC.

- *Scheme 3: same tx power level.* This is the simplest scheme. It consists of setting a fixed level of transmission power for every node, i.e.,  $P_{tx,i} = P_{tx,\max}$ ,  $\forall i$ . Every node is able to use this power level regardless of its position and channel conditions.

### C. Interference and SIC

The SINR of node  $i$ , denoted with  $\Gamma_i$  can be written as follows:

$$\Gamma_i = \frac{G_{d,i} G_{s,i} G_{f,i} P_{tx,i}}{P_N + P_{I,i}} = \frac{G_{d,i} G_{s,i} G_{f,i} P_{tx,i}}{P_N + \sum_{j \neq i} G_{d,j} G_{s,j} G_{f,j} P_{tx,j}} \quad (6)$$

Note that these SINR equations should be considered with different power adaption schemes, as described in previous subsection.

MPR is based on an information-theoretic framework [1]. Perfect interference cancellation is assumed with SIC, unless otherwise explicitly stated.

Let us assume that  $k$  packet are received simultaneously and let  $S_j$ ,  $j = 1, \dots, k$  be their respective SNR levels. Assume they are ordered in descending order, i.e.,  $S_1 \geq S_2 \dots \geq S_k$  (ties are broken at random). SIC works as follows. Provided decoding of packets  $1, \dots, h-1$  be successful, packet  $h$  is decoded successfully if and only if its SINR, accounting only for *residual* interference after cancellation, exceeds the threshold  $\gamma$ :

$$\frac{S_h}{1 + \sum_{r=h+1}^k S_r} \geq \gamma \quad (7)$$

For comparison purposes, we consider a baseline receiver that can only exploit the capture effect, i.e., it is able to decode packet  $h$  successfully only in case its SINR, accounting for interference from *all* concurrent transmissions, exceeds the threshold  $\gamma$ :

$$\frac{S_h}{1 + \sum_{r=1, r \neq h}^k S_r} \geq \gamma \quad (8)$$

For imperfect SIC, a parameter  $\xi \in [0, 1]$  is introduced, which represents the fraction of residual uncanceled transmission power. Then, Equation (7) modifies to:

$$\frac{S_h}{1 + \sum_{r=h+1}^k S_r + \xi \sum_{j=1}^{h-1} S_j} \geq \gamma \quad (9)$$

Perfect interference cancellation corresponds to the case  $\xi = 0$ , while  $\xi = 1$  boils down to the baseline receiver.

#### D. Sum-rate analysis

The overall sum-rate,  $U$ , is defined as, average delivered data bit per unit of time/channel bandwidth.

By standard argument [1], it is shown that the overall sum-rate  $U$  in case of Slotted ALOHA is given by

$$U = \log_2(1 + \gamma) \sum_{k=1}^n m_k \binom{n}{k} p^k (1-p)^{n-k} \quad (10)$$

where  $m_k$  is the mean number of successfully decoded packets in a slot, conditional on  $k$  nodes attempting their transmissions. In case of CSMA the overall sum-rate is expressed as follows:

$$U = \log_2(1 + \gamma) \frac{\sum_{k=1}^n m_k \binom{n}{k} p^k (1-p)^{n-k}}{\beta + 1 - (1-p)^n} \quad (11)$$

where  $\beta = \delta/T$  is the normalized back-off time slot duration. Note that we assume  $\delta$  is a constant, and does not scale with  $\gamma$ . As a consequence,  $\beta$  varies with  $\gamma$ , since  $T$  varies with  $\gamma$ .

In the following, we set the transmission probability  $p$  to the value that maximizes the mean number of packets delivered per slot, for each value of  $\gamma$ .

Table I  
SIMULATION PARAMETERS.

Parameters	Value	Parameters	Value
$P_{tx,min}$	-20 dBm	$P_{tx,max}$	20 dBm
$h_{tx}$	2 m	$h_{rx}$	8 m
$F_N$	5 dB	$W$	1 MHz
$\sigma_s$	8 dB	$L$	2000 bits
$\delta$	100 $\mu$ s		

## IV. PERFORMANCE EVALUATION

The presented analytical models are validated against MATLAB simulations by implementing the MAC layer protocols slotted ALOHA, and CSMA along with system model assumptions defined in Section III. The results are divided into different section based on system model settings described in Section III.

The sum-rate performance metric introduced in Section III-D is plotted as a function of the SINR threshold  $\gamma$ . We consider a quite stretched range of values of  $\gamma$  mainly for the purpose of highlighting the existence of different operational regimes of the system. Numerical values of main system parameter are listed in Table I.

We consider four combinations of multiple access schemes: SA and CSMA at MAC layer, and receiver with SIC or without SIC (i.e., only capture effect is in place). Curves referring to SA are colored in blue, CSMA curves are red. Curves referring to SIC are plotted as solid lines, capture only (without SIC) being plotted as dashed line curves.

#### A. Basic Model Evaluation

In this subsection we recap a few results from [1], with the path loss model introduced in subsection III-A. The results presented in this subsection are specific to power control *scheme 1* introduced in subsection III-B.

The mean number of correctly decoded packets in one transmission time,  $m_k$ , conditional on  $k$  nodes transmitting, is shown in Figure 1 as a function of  $\gamma$ , in case of capture effect only (no SIC). Figure 2 shows  $m_k$  in case of SIC. Both these figures are shown for several values of  $k$ .

In both cases,  $m_k$  is monotonously decreasing with  $\gamma$ , which is quite intuitive, since higher values of  $\gamma$  are more challenging for the receiver.

Another common feature of  $m_k$  plots is that  $m_1 > m_k, \forall k > 1$ , for sufficiently large values of  $\gamma$ , both with and without SIC. This shows that it is best to avoid concurrent transmissions in high spectral efficiency regime (large  $\gamma$ ). On the contrary, for small  $\gamma$  values, the higher  $k$ , the bigger the number of correctly decoded packets. In fact, for very low  $\gamma$  values, interference cancellation is quite effective and even capture works fine for many packets. The main difference between the results with SIC and without SIC lies with the behavior of curves for intermediate values of  $\gamma$ . The transition in case of SIC is much sharper than in the other case, denoting a sort of threshold effect.

Figure 3 shows the optimal value of the transmission probability  $p$  as a function of  $\gamma$ . For low SINR threshold values,

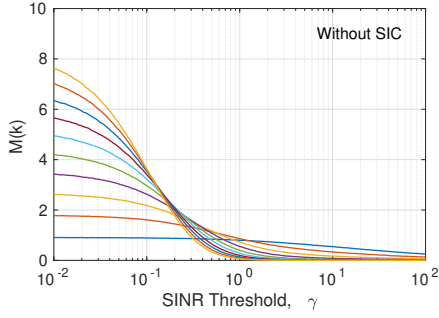


Figure 1. Mean number of correctly decoded packets conditional on  $k$  nodes transmitting,  $m_k$ , as a function of SINR threshold  $\gamma$ , in case of capture effect only.

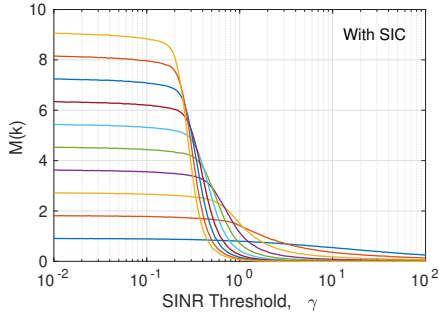


Figure 2. Mean number of correctly decoded packets conditional on  $k$  nodes transmitting,  $m_k$ , as a function of SINR threshold  $\gamma$ , in case of SIC at the receiver.

physical layer (SIC) is mainly responsible for improving the system performance while the role of MAC layer is negligible, because all the nodes are allowed to transmit simultaneously, i.e., the optimal transmission probability is 1. For large values of  $\gamma$ , the MAC layer is the bottleneck, since the collisions are mainly responsible for the performance degradation. Hence the optimal value of  $p$  becomes smaller and smaller as  $\gamma$  grows. This effect is also clear in the sum-rate plot in Figure 4.

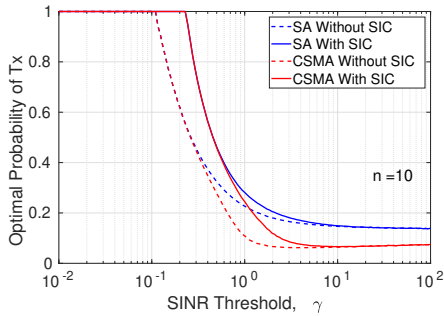


Figure 3. Optimal value of the transmission probability  $p$  as a function of SINR threshold  $\gamma$ .

Two peaks appear in Figure 4, one in the low  $\gamma$  range and another one in the high  $\gamma$  range. As for capture only performance, the highest sum-rate is achieved for relatively high values of  $\gamma$ , while low spectral efficiency operation leads

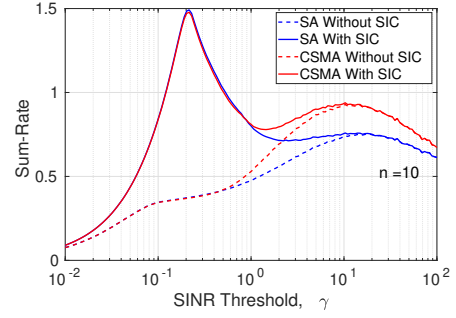


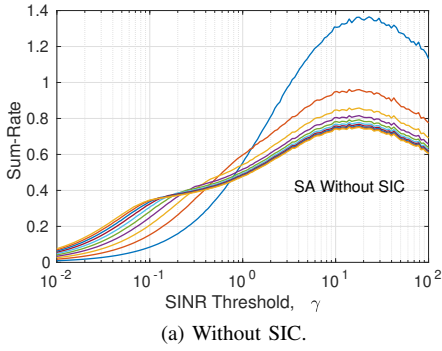
Figure 4. Sum-Rate  $U$  as a function of SINR threshold  $\gamma$  for the optimized value of the transmission probability  $p$ .

to very low sum-rate values. Moreover, CSMA turns out to offer superior sum-rate performance with respect to SA, which is a well known classic result. The peak of sum-rate shows that essentially the same performance is achieved with and without SIC. In other words, when working in the high spectral efficiency regime (high values of  $\gamma$ ), SIC provides little gain to random access protocols in terms of throughput. Note that the high spectral efficiency regime is the typical choice of cellular system as well as WiFi.

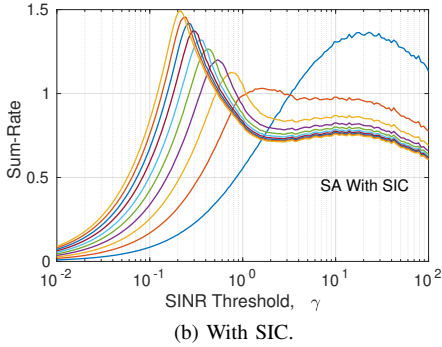
In case of SIC, a second peak of sum-rate appears for lower values of  $\gamma$ , i.e., when the system is operated in a low spectral efficiency regime. This is the region of choice of, e.g., spread-spectrum systems, or of some sensor network technology, e.g., LoRaWAN. The same optimized performance is achieved by SA and CSMA at this left peak of sum-rate, which is consistent with the fact that the optimal value of the transmission probability is 1 or close to 1, so that the MAC protocol plays essentially no role. On the contrary, SIC has a major effect on performance for low values of  $\gamma$ . When only capture effect is exploited (no SIC), the achieved sum-rate is very low, definitely worse than what can be achieved at high  $\gamma$  values. If SIC is in place, a strong improvement of sum-rate is obtained, even better than what is achieved for large  $\gamma$ .

Based on this brief recap, now we highlight the sensitivity of sum-rate in the two identified regimes, with respect to the number of contending nodes  $n$ . The sum-rate with and without SIC for several values of the number of nodes  $n$  is shown in Figures 5 and 6 in case of SA and CSMA respectively.

These plots provide valuable insight into the system working as the number of nodes is varied. When there is only one node there is no point to use low spectral efficiency, As the number of contending nodes  $n$  increases, using high values of  $\gamma$  and limiting the number of concurrent transmission by reducing  $p$  is the best strategy without SIC. On the contrary, with SIC, the sum-rate peak in low spectral efficiency regime moves to the left, while the sum-rate peak in the high spectral efficiency regime fades away, due to collisions. The SIC-enabled PHY layer allow most or all nodes to transmit, but at the same time it forces nodes to pick low  $\gamma$  values to get decoded successfully. The optimal  $\gamma$  providing the sum-rate peak decreases as  $n$  grows. In this low threshold regime there is no need of MAC



(a) Without SIC.



(b) With SIC.

Figure 5. Sum-Rate  $U$  as a function of SINR threshold  $\gamma$  for the optimized value of the transmission probability  $p$ , for several values of the number of nodes  $n$ .

regulation. Grant-free transmissions can be enabled by means of SIC thanks to its MPR capability.

### B. Power Control Evaluation

*Scheme 2* and *Scheme 3* defined in Section III-B, are evaluated in this subsection. Results with *Scheme 1* have been displayed in Section IV-A.

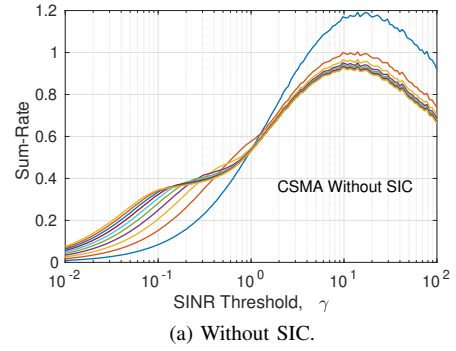
Figure 7 plots the sum-rate as a function of  $\gamma$ , where the transmission power  $P_{tx}$  is proportional to the distance from the BS (*scheme 2*). The overall sum-rate in the low threshold regime is increased significantly, which is quite intuitive as we are inducing a great difference in the received power levels with respect to *scheme 1* and SIC is exploiting this difference to decode more packets successfully.

The sum-rate performance obtained by adopting power control *scheme 3*, shown in Figure 8, lead to only a slight improvement over the sum-rate obtained by adopting *scheme 2*. However, using the maximum transmission power level at all nodes will induces a higher energy cost, which appears to be unwarranted, given the marginal benefit in terms of sum-rate.

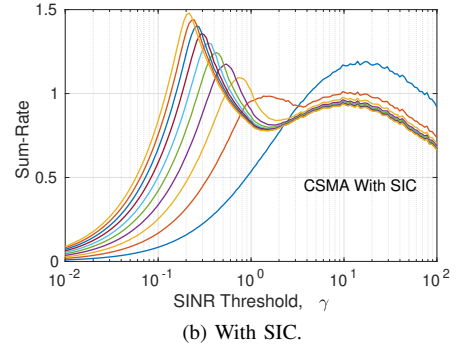
The sum-rate performance given by power control *scheme 1*, shown in Figure 4, is significantly lower than the other two considered power schemes. This is expected, since *Scheme 1* strives for equalizing received power levels, forbidding power differences exploited by SIC.

### C. Imperfect interference cancellation

In this subsection we identify the impact of imperfect interference cancellation in case of *scheme 1* of power control.



(a) Without SIC.



(b) With SIC.

Figure 6. Sum-Rate  $U$  as a function of SINR threshold  $\gamma$  for the optimized value of the transmission probability  $p$ , for several values of the number of nodes  $n$ .

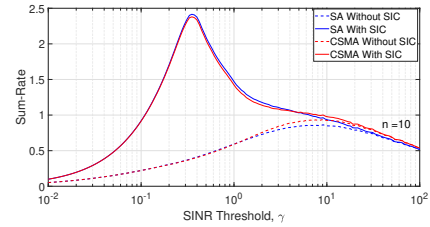


Figure 7. Sum-Rate  $U$  as a function of SINR threshold  $\gamma$  for the optimized value of the transmission probability  $p$  ( $P_{tx}$  changes with respect to node positions).

Similar results are obtained in case of *scheme 2* and *scheme 3* in terms of reduction of sum-rate performance achieved by each scheme with perfect cancellation.

Figure 9 shows the sum-rate as a function of  $\gamma$  for  $n = 10$  nodes, always backlogged, and for several values of the residual interference coefficient  $\xi$ , ranging between 0 (perfect cancellation) up to 1 (no cancellation at all, i.e., no SIC).

It shows that even 10-20% of residual interference causes a strong degradation of the sum-rate performance. This results hint at the requirement of a highly accurate interference cancellation to reap a substantial sum-rate gain in low spectral efficiency regime with respect to high spectral efficiency regime.

This analysis is summarized in Figure 10, where the mean number of successfully decoded packets given that  $k$  nodes transmit simultaneously,  $m_k$ , is plotted for  $k = 10$  and  $\gamma =$

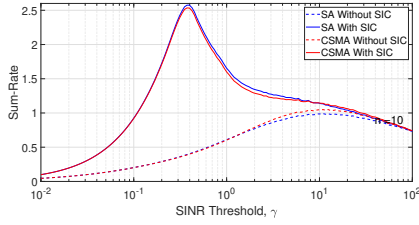
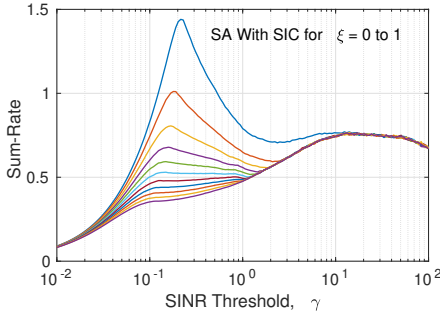
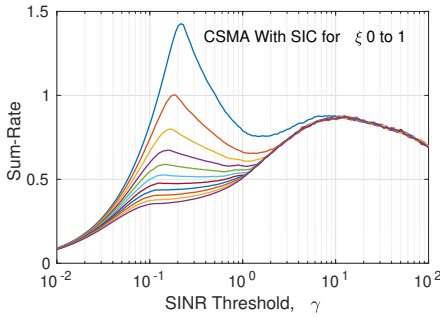


Figure 8. Sum-Rate  $U$  as a function of SINR threshold  $\gamma$  for the optimized value of the transmission probability  $p$  ( $P_{tx}$  is fixed for all nodes).



(a) Slotted ALOHA.



(b) CSMA.

Figure 9. Sum-Rate  $U$  in case of imperfect interference cancellation as a function of SINR threshold  $\gamma$  for the optimized value of the transmission probability  $p$  and for several values of the interference cancellation factor  $\xi$ .

0.2 as a function of  $\xi$ . The main result here is how fast the degradation of performance occurs when we change  $\xi$ . This confirms that a very accurate SIC is required to work in this low spectral efficiency regime.

## V. DYNAMIC OPTIMIZATION

In this section we address the dynamic optimization of the SIC-based multiple access system considered so far in a non-saturated environment. To keep the analysis simple, we confine ourselves to the first transmission power setting scheme, and we relax the transmission power limits to  $P_{tx,max} = \infty$  and  $P_{tx,min} = 0$ . As a result, the received SNR of nodes that transmit in a slot are negative exponential random variables, with mean  $S_0 = \gamma / (-\log(1 - \epsilon))$ .

Time is slotted with variable size slots. The duration of time slot  $t$  is denoted with  $T(t)$ , for  $t = 1, 2, \dots$

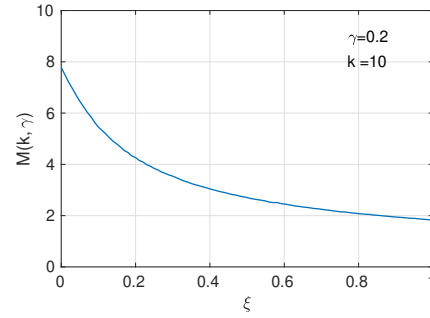


Figure 10. Mean number of correctly decoded packets conditional on  $k$  nodes transmitting simultaneously as a function of Interference Cancellation factor  $\xi$ , for  $k = 10$  and  $\gamma = 0.2$ .

At the beginning of slot  $t$ , a target SINR  $\gamma(t)$  and a transmission probability for backlogged nodes  $p(t)$  are set. Nodes adjust their transmitting power and coding scheme to conform to the required SINR  $\gamma(t)$  in slot  $t$ . Hence, the duration of the slot is

$$T(t) = \frac{L}{W \log_2(1 + \gamma(t))} \quad (12)$$

Decoding of concurrently transmitted messages occurs by using SIC, as described in Section III-C. Let  $Y_j$  denote the received SNR of transmitting node  $j$ , when  $k$  nodes transmit in slot  $t$ . Note that  $k$  is the outcome of binomial random variable with parameters  $n$  and  $p(t)$ , if  $n$  nodes are backlogged at the beginning of slot  $t$ . We can write  $Y_j = S_0 X_j$ , where  $X_j$  is a negative exponential random variable with mean 1, accounting for Rayleigh fading. Assume the SNRs are sorted so that  $Y_1 \geq Y_2 \geq \dots \geq Y_k$ . Then decoding of the data sent by node  $j$  is successful if all packets sent by nodes  $i < j$  have been decode successfully (and hence their interference has been cancelled) and

$$\frac{S_j}{1 + \sum_{h=j+1}^k S_h} \geq \gamma(t) \quad \Rightarrow \quad X_j \geq c + \gamma(t) \sum_{h=j+1}^k X_h \quad (13)$$

where  $c = -\log(1 - \epsilon)$ .

We assume an infinite population of nodes shares the channel. Nodes become backlogged upon message generation. Globally, new messages are generated by the node population according to a Poisson process with mean arrival rate  $\lambda$ .

A backlogged node contends the channel according to a Slotted ALOHA algorithm with transmission probability  $p(t)$  in time slot  $t$ . A transmitting node will know the outcome of its transmission attempt by the end of the slot where it has transmitted. In case of failure, the node will re-schedule the message or make a new transmission attempt, until it is eventually delivered to the BS successfully. At that point the node goes back into the population of idle nodes. If no node transmits in one slot, the slot has a fixed duration  $T_{oh} = 1$  ms.

The time evolution of the number of backlogged nodes is described by the following dynamics

$$Q(t+1) = Q(t) + A(t) - D(t) \quad (14)$$

where

- $Q(t)$  is the number of nodes that are backlogged at the beginning of slot  $t$ .
- $A(t)$  is the number of nodes that become backlogged in slot  $t$ .
- $D(t)$  is the number of packets that are successfully decoded, hence acknowledged, by the BS in slot  $t$ .

Given that arrivals on new nodes follows a Poisson process, the mean of  $A(t)$ , conditional on  $Q(t) = n$ , is given by

$$\mathbb{E}[A(t) | Q(t) = n] = \lambda T(t) \quad (15)$$

where  $T(t)$  is given in Equation (12).

The mean of  $D(t)$ , conditional on  $Q(t) = n$ , is

$$\mathbb{E}[D(t) | Q(t) = n] = \sum_{k=0}^n m_k(\gamma(t)) \binom{n}{k} [p(t)]^k [1 - p(t)]^{n-k} \quad (16)$$

where  $m_k(\gamma)$  is the mean number of packets successfully decoded, when  $k$  nodes transmit and the target SINR is  $\gamma$ . For ease of notation, we include the case  $k = 0$  and set  $m_0(\cdot) = 0$ .

The conditional drift of the system described by Equation (14) is

$$\Delta(t) = \mathbb{E}[A(t) | Q(t) = n] - \mathbb{E}[D(t) | Q(t) = n] \quad (17)$$

For  $\Delta(t)$  to be negative, it must be

$$\lambda < \frac{W}{L} U(p(t), \gamma(t)) \quad (18)$$

where  $U = U(p(t), \gamma(t))$  is given by

$$U = \log_2(1 + \gamma(t)) \sum_{k=0}^n m_k(\gamma(t)) \binom{n}{k} [p(t)]^k [1 - p(t)]^{n-k} \quad (19)$$

It is the sum rate in slot  $t$ , given that  $Q(t) = n$  and system parameters are set to  $\gamma(t)$  and  $p(t)$ .

To guarantee stability (which requires negative drift) and optimize the efficiency of the system, we assume that  $p(t)$  and  $\gamma(t)$  are set so as to maximize  $U$  in each time slot. Formally, given that  $Q(t) = n$ , we set  $\gamma(t) = \gamma^*(n)$  and  $p(t) = p^*(n)$ , where  $\gamma^*(n)$  and  $p^*(n)$  are the values of  $\gamma$  and  $p$  that maximize  $U$  in time slot  $t$ .<sup>1</sup>

Numerical evaluation suggests that, as  $n$  grows, we have  $\gamma^*(n) \sim 1/(a_\gamma n)$ , with  $a_\gamma \approx 0.382$ ,  $p^*(n) \sim 1$ , and  $m_n(\gamma^*(n)) \sim a_m n$ , with  $a_m \approx 0.859$

Plots of  $\gamma^*(n)$  and  $p^*(n)$  as a function of  $n$  for  $\epsilon = 0.1$  are shown in Figures 11a and 11b respectively. The target SINR is normalized to its maximum allowed value  $\gamma_{\max} = 100$ . The asymptotic behavior that has been extrapolated numerically from simulation experiments are shown with a red dashed line. It is noted that a critical cut-off exists  $N_c = 12$ . For  $n \leq N_c$  the maximum sum rate is achieved by the high spectral efficiency regime, hence the best parameter setting is choosing the maximum allowed value of  $\gamma$  and letting  $p^*(n) = 1/n$ , so

<sup>1</sup>It can be shown that this setting is consistent with what would come from the application of Lyapunov drift stochastic optimization applied to the dynamic system Equation (14), according to [29, Ch. 7].

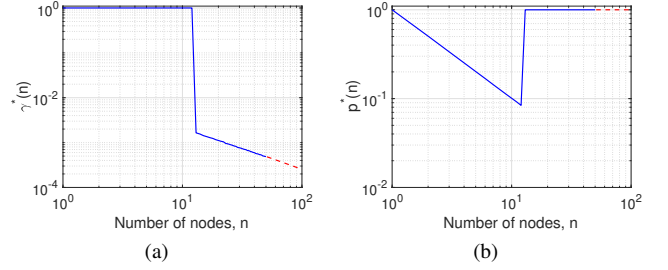


Figure 11. Value of system parameters that maximizes the sum rate when  $n$  nodes are backlogged, for  $\epsilon = 0.1$ . (a) Normalized target SINR  $\gamma^*(n)/\gamma_{\max}$ , with  $\gamma_{\max} = 100$ . (b) Probability of transmission  $p^*(n)$ .

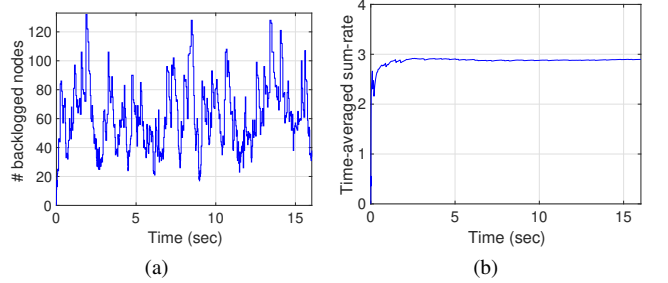


Figure 12. (a) Evolution of number of backlogged nodes,  $Q(t)$ , as a function of time, obtained with optimal target SINR and transmission probability. (b) Time average sum-rate.

that the expected number of transmitting nodes is 1. For  $n > N_c$ , the sum rate is maximizing by working in the low spectral efficiency region, hence  $p^*(n) = 1$  and  $\gamma^*(n)$  is inversely proportional to  $n$ .

Asymptotically as  $n \rightarrow \infty$ , it follows that  $U$ , under optimal choice of  $\gamma$  and  $p$ , tends to

$$U(p^*(n), \gamma^*(n)) \sim \log_2 \left( 1 + \frac{1}{a_\gamma n} \right) m_n(\gamma^*(n)) \sim \frac{a_m}{a_\gamma \log 2} \quad (20)$$

We get  $\lim_{n \rightarrow \infty} U(p^*(n), \gamma^*(n)) \approx 3.25 \equiv U_\infty$ . To guarantee stability we require therefore that  $\lambda < WU_\infty/L$ . In the following, we set

$$\lambda = \rho \frac{WU_\infty}{L} \quad (21)$$

where  $\rho < 1$  is a load parameter.

Simulations of the optimized system have been run with  $L = 2000$  bit,  $W = 1$  MHz,  $\rho = 0.9$ ,  $\epsilon = 0.1$ . The time evolution of a sample path of  $Q(t)$ , starting from  $Q(0) = 0$ , is shown in Figure 12a.

Let the cumulative time average sum rate be defined as

$$\bar{U}(t) = \frac{1}{t} \sum_{\tau=1}^t U(\tau) \quad (22)$$

where  $U(t) = \log(1 + \gamma(t))\mathbb{E}[D(t)]$ . Figure 12b shows  $\bar{U}(t)$  as a function of time, obtained with optimal target SINR and transmission probability. It is apparent from those plots that the queue is under control (fluctuations do not diverge) and the time-averaged sum rate tends to 90% of its asymptotic



value ( $0.9 \cdot 3.25 = 2.925$ ), which is the maximum that can be obtained, given the load  $\rho = 0.9$ .

## VI. CONCLUSION

We have presented a comprehensive analysis of SA and CSMA with SIC-enabled physical layer in terms of sum-rate. First we highlight the existence of two working regimes, where the sum-rate metric exhibit relative maxima.

Different schemes are used for transmission power setting at nodes, under the constraint of a finite power dynamic range. Main results are as follows: (i) sum-rate improves, if received power levels are different for nodes transmitting simultaneously; (ii) highly accurate interference cancellation is required to operate in the low spectral efficiency regime effectively.

Finally, we outline a dynamic algorithm to select the target SINR and the transmission probability in case of varying number of backlogged nodes. The algorithm attains the maximum possible sum-rate, provided the system can be stabilized, i.e., it is throughput optimal, where throughput is identified with sum-rate.

The takeaway of this study is the possibility of designing massive multiple access for large population of nodes that send infrequent messages based on SIC rather than standard random access protocols. A critical issue highlighted in this work is that accurate interference cancellation is required. As future work, we aim to design a distributed adaptive algorithm that leverages on the dynamic optimization framework introduced in this paper. Moreover, practical coding schemes and processing algorithms to achieve SIC should be investigated as well.

## ACKNOWLEDGMENT

This work was partially supported by the European Union under the Italian National Recovery and Resilience Plan (NRRP) of Next Generation EU, partnership on “Telecommunications of the Future” (PE00000001 - program “RESTART”).

## REFERENCES

- [1] A. B. Abdul Razzaque, H. K. Qureshi, and A. Baiocchi, “Low vs high spectral efficiency communications with sic and random access,” in *2022 IEEE 11th IFIP International Conference on Performance Evaluation and Modeling in Wireless and Wired Networks (PEMWN)*, 2022, pp. 1–6.
- [2] A. Rajandekar and B. Sikdar, “A survey of mac layer issues and protocols for machine-to-machine communications,” *IEEE Internet of Things Journal*, vol. 2, no. 2, pp. 175–186, 2015.
- [3] M. Chafii, L. Bariah, S. Muhaidat, and M. Debbah, “Twelve scientific challenges for 6g: Rethinking the foundations of communications theory,” *IEEE Communications Surveys & Tutorials*, vol. 25, no. 2, pp. 868–904, 2023.
- [4] K. Zheng, S. Ou, J. Alonso-Zarate, M. Dohler, F. Liu, and H. Zhu, “Challenges of massive access in highly dense lte-advanced networks with machine-to-machine communications,” *IEEE Wireless Communications*, vol. 21, no. 3, pp. 12–18, 2014.
- [5] M. B. Shahab, R. Abbas, M. Shirvanimoghaddam, and S. J. Johnson, “Grant-free non-orthogonal multiple access for iot: A survey,” *IEEE Communications Surveys & Tutorials*, vol. 22, no. 3, pp. 1805–1838, 2020.
- [6] Y. Liu, S. Zhang, Z. Ding, R. Schober, N. Al-Dhahir, E. Hossain, and X. Shen, “Special Issue on Next Generation Multiple Access—Part I,” *IEEE Journal on Selected Areas in Communications*, vol. 40, no. 4, pp. 1031–1036, 2022.
- [7] Y. Liu, S. Zhang, X. Mu, Z. Ding, R. Schober, N. Al-Dhahir, E. Hossain, and X. Shen, “Evolution of NOMA Toward Next Generation Multiple Access (NGMA) for 6G,” *IEEE Journal on Selected Areas in Communications*, vol. 40, no. 4, pp. 1037–1071, 2022.
- [8] Y. Mao, O. Dizdar, B. Clerckx, R. Schober, P. Popovski, and H. V. Poor, “Rate-Splitting Multiple Access: Fundamentals, Survey, and Future Research Trends,” *IEEE Communications Surveys & Tutorials*, vol. 24, no. 4, pp. 2073–2126, 2022.
- [9] J.-B. Seo, B. C. Jung, and H. Jin, “Performance analysis of noma random access,” *IEEE Communications Letters*, vol. 22, no. 11, pp. 2242–2245, 2018.
- [10] J. Choi, “Noma-based random access with multichannel aloha,” *IEEE Journal on Selected Areas in Communications*, vol. 35, no. 12, pp. 2736–2743, 2017.
- [11] —, “On throughput bounds of NOMA-ALOHA,” *CoRR*, vol. abs/2110.12530, 2021.
- [12] H. Lin, K. Ishibashi, W.-Y. Shin, and T. Fujii, “A simple random access scheme with multilevel power allocation,” *IEEE Communications Letters*, vol. 19, no. 12, pp. 2118–2121, 2015.
- [13] C. Xu, L. Ping, P. Wang, S. Chan, and X. Lin, “Decentralized power control for random access with successive interference cancellation,” *IEEE Journal on Selected Areas in Communications*, vol. 31, no. 11, pp. 2387–2396, 2013.
- [14] Y. Li and L. Dai, “Maximum sum rate of slotted aloha with successive interference cancellation,” *IEEE Transactions on Communications*, vol. 66, no. 11, pp. 5385–5400, 2018.
- [15] A. K. Gupta, T. G. Venkatesh, and N. Vuppapapati, “Sic and csi-based random channel access protocol for wlan supporting multi packet transmission,” in *2022 IEEE Global Conference on Artificial Intelligence and Internet of Things (GCAIoT)*, 2022, pp. 188–193.
- [16] M. Shirvanimoghaddam, M. Dohler, and S. J. Johnson, “Massive non-orthogonal multiple access for cellular iot: Potentials and limitations,” *IEEE Communications Magazine*, vol. 55, no. 9, pp. 55–61, 2017.
- [17] Z. Dawy, W. Saad, A. Ghosh, J. G. Andrews, and E. Yaacoub, “Toward massive machine type cellular communications,” *IEEE Wireless Communications*, vol. 24, no. 1, pp. 120–128, 2017.
- [18] J. Choi, J. Ding, N.-P. Le, and Z. Ding, “Grant-free random access in machine-type communication: Approaches and challenges,” *IEEE Wireless Communications*, vol. 29, no. 1, pp. 151–158, 2022.
- [19] N. H. Mahmood, R. Abreu, R. Böhnke, M. Schubert, G. Berardinelli, and T. H. Jacobsen, “Uplink grant-free access solutions for urllc services in 5g new radio,” in *2019 16th International Symposium on Wireless Communication Systems (ISWCS)*, 2019, pp. 607–612.
- [20] Z. Ding, R. Schober, P. Fan, and H. V. Poor, “Simple semi-grant-free transmission strategies assisted by non-orthogonal multiple access,” *IEEE Transactions on Communications*, vol. 67, no. 6, pp. 4464–4478, 2019.
- [21] C. Zhang, Y. Liu, and Z. Ding, “Semi-grant-free noma: A stochastic geometry model,” *IEEE Transactions on Wireless Communications*, vol. 21, no. 2, pp. 1197–1213, 2022.
- [22] S. A. Tegos, P. D. Diamantoulakis, A. S. Lioumpas, P. G. Sarigiannidis, and G. K. Karagiannidis, “Slotted aloha with noma for the next generation iot,” *IEEE Transactions on Communications*, vol. 68, no. 10, pp. 6289–6301, 2020.
- [23] S. M. R. Islam, N. Avazov, O. A. Dobre, and K.-s. Kwak, “Power-domain non-orthogonal multiple access (noma) in 5g systems: Potentials and challenges,” *IEEE Communications Surveys & Tutorials*, vol. 19, no. 2, pp. 721–742, 2017.
- [24] J.-L. Lu, W. Shu, and M.-Y. Wu, “A Survey on Multi-packet Reception for Wireless Random Access Networks,” *Journal of Computer Networks and Communications*, July 2012.
- [25] M. Ivanov *et al.*, “Broadcast Coded Slotted ALOHA: A Finite Frame Length Analysis,” *IEEE Trans. on Communications*, vol. 65, no. 2, Feb 2017.
- [26] F. Ricciato and P. Castiglione, “Pseudo-random Aloha for Enhanced Collision-recovery in RFID,” *IEEE Comm. Letters*, vol. 17, no. 3, March 2013.
- [27] Y. Li and L. Dai, “Maximum sum rate of slotted aloha with capture,” *IEEE Transactions on Communications*, vol. 64, pp. 1–1, 01 2015.
- [28] C. Sommer, S. Joerer, and F. Dressler, “On the applicability of two-ray path loss models for vehicular network simulation,” in *2012 IEEE Vehicular Networking Conference (VNC)*, 2012, pp. 64–69.
- [29] M. J. Neely, *Stochastic Network Optimization with Application to Communication and Queueing Systems*. Morgan & Claypool, 2010.